Batch studies of phosphonate adsorption on granular ferric hydroxides

T. Reinhardt, M. Gómez Elordi, R. Minke, H. Schönberger and E. Rott

ABSTRACT

Phosphonates are widely used in various industries. It is desirable to remove them before discharging phosphonate-containing wastewater. This study describes a large number of batch experiments with adsorbents that are likely suitable for the removal of phosphonates. For this, adsorption isotherms for four different granular ferric hydroxide (GFH) adsorbents were determined at different pH values in order to identify the best performing material. Additionally, the influence of temperature was studied for this GFH. A maximum loading for nitrilotrimethylphosphonic acid (NTMP) was found to be ~12 mg P/g with an initial concentration of 1 mg/L NTMP-P and a contact time of 7 days at room temperature. Then, the adsorption of six different phosphonates was investigated as a function of pH. It was shown that GFH could be used to remove all investigated phosphonates from water and, with an increasing pH, the adsorption capacity decreased for all six phosphonates. Finally, five adsorption–desorption cycles were carried out to check the suitability of the material for multiple re-use. Even after five cycles, the adsorption process still performed well.

Key words | desorption, DTPMP, GFH, HEDP, NTMP, PBTC

T. Reinhardt (corresponding author)
M. Gómez Elordi
R. Minke
H. Schönberger
E. Rott
Institute for Sanitary Engineering, Water Quality and Solid Waste Management,
University of Stuttgart,
Bandtäle 2, 70569 Stuttgart,
Germany
E-mail: *tobias.reinhardt@iswa.uni-stuttgart.de*

INTRODUCTION

The worldwide limits for the discharge of phosphorus into water bodies are becoming increasingly stringent. With regard to phosphorus emission, in addition to ortho-phosphate, other quantitatively relevant P-containing compounds such as phosphonates should be considered (Figure 1). Phosphonates are complexing agents that are used in domestic detergents, but also in various industries, such as in the textile industry as bleach stabilizers, in drinking water purification as antiscalants, and in industrial detergents (Nowack & Stone 1999a; Boels *et al.* 2012). In only 14 years (1998–2012), the global phosphonate consumption grew by more than 67% from 56,000 t/a to 94,000 t/a (Davenport *et al.* 2000 (cited by Nowack 2003); EPA 2013).

Phosphonates are suspected of contributing to the eutrophication of water bodies, as UV radiation can promote their degradation to readily available ortho-phosphate (Matthijs *et al.* 1989; Lesueur *et al.* 2005; Kuhn *et al.* 2018; Rott *et al.* 2018a). Only recent developments in phosphonate analytics have shown that phosphonates accumulate significantly in sediments and suspended solids and, therefore, could lead to long-term environmental impacts (Armbruster *et al.* 2019).

With regard to the removal of phosphonates from wastewater, the use of UV lamps is often limited due to high energy costs and an inability to treat the incoming large volumes of wastewater. During the Fenton and flocculation process, large quantities of sludge are produced, which then must be separated and disposed of expensively. In addition, a very high flocculant concentration is often required to form a sufficient amount of flocs, as phosphonates are very strong complexing agents (Rott *et al.* 2017a, 2017b).

A possible alternative for the removal of phosphonates is to use iron-containing filter materials as this utilizes their high adsorption affinity towards metal-containing surfaces. Possible adsorbents range from iron-coated sand (Boels *et al.* 2010) and commercially available granular ferric hydroxides (GFH) (Boels *et al.* 2012; Chen *et al.* 2017) to engineered composite particles (Rott *et al.* 2018b) and minerals such as goethite (Nowack & Stone 1999a). These adsorbents must have both a high adsorption capacity and an effective regenerability for them to be applicable in large-scale wastewater treatment applications.

doi: 10.2166/wst.2020.055

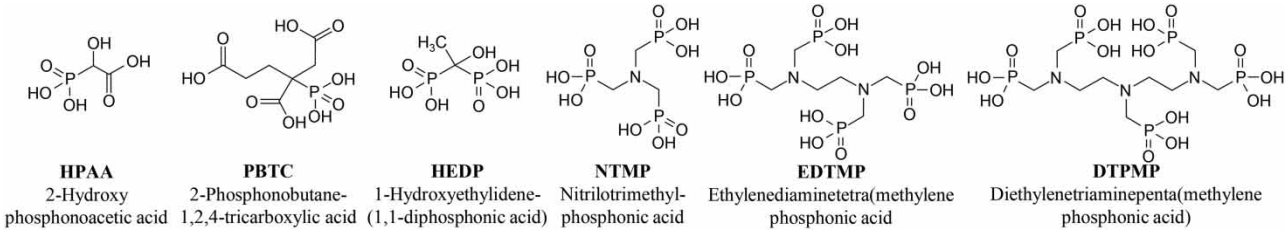

Figure 1 | Chemical structures of considered phosphonates.

So far, however, hardly any studies have been published on these properties with regard to iron-containing adsorbents and phosphonates. Furthermore, only one phosphonate is investigated in these studies, although various phosphonates with different properties are used in industrial processes. For instance, an intensive literature search has not revealed any previous investigations on the removal of HPAA. Therefore, in order to close the knowledge gaps mentioned above, this study describes a large number of batch experiments with four different GFH adsorbents likely suitable for the removal of phosphonates.

MATERIALS AND METHODS

Reagents and chemicals

All solutions were prepared with deionized water produced from drinking water using an ion exchanger (Seradest SD 2000) and a filter unit (Seralpur PRO 90 CN). Acetic acid (AcOH) (100%, Ph. Eur.) and hydrochloric acid (32%, AnalaR NORMAPUR) were obtained from VWR Chemicals (Fontenay-sous-Bois, France) and NaOH (≥99%, Ph. Eur.) from Merck (Darmstadt, Germany); 2-(*N*-morpholino)-ethanesulfonic acid (MES) (≥99%), 3-(*N*-morpholino)-propanesulfonic acid (MOPS) (≥99.5%), 4-(2-hydroxyethyl)-1-piperazinepropanesulfonic acid (EPPS) (≥99.5%), 3-(cyclohexylamino)-2-hydroxy-1-propanesulfonic acid (CAPSO) (≥99.5%), 3-(cyclohexylamino)-1-propanesulfonic acid (CAPS) (≥98%), HEDP·H_2O (≥95%), and NTMP (≥97%) originated from SigmaAldrich (St Louis, MO, USA). PBTC, as a technical solution (50%, CUBLEN P 50), as well as EDTMP (5.3% water of crystallization) and DTPMP (16% water of crystallization), both as solids, were obtained from Zschimmer & Schwarz Mohsdorf (Burgstädt, Germany). HPAA, as a technical solution (50%), was purchased from Connect Chemicals (Ratingen, Germany).

Adsorbents

A total of four different GFH adsorbents were investigated, with their properties shown in Table 1 and macro photographs depicted in Figure 2. Each adsorbent was rinsed once with distilled water over a sieve until the water was clear and then air-dried under a fume hood.

Experimental procedure

Buffered solutions containing 1 mg/L P for the six phosphonates in Figure 1 were prepared as follows (pH target value (pH_{start}) with buffer concentration in brackets): pH 4 (0.01 M AcOH), pH 5 (0.01 M AcOH), pH 6 (0.01 M MES), pH 7 (0.01 M MOPS), pH 8 (0.01 M EPPS), pH 9 (0.01 M CAPSO), pH 10 (0.01 M CAPS), and pH 12 (0.01 M CAPS). The pH was set using HCl or NaOH. The required amount of adsorbent was weighed into a 50 mL centrifuge tube, which was then filled with the buffered P-containing solution to the 50 mL mark, immediately closed, and clamped in the overhead rotator running at 20 rpm (LLG-uniROTATOR 2). After the predefined contact time, the centrifuge tube was promptly removed and a volume of approximately 20 mL of the supernatant was

Table 1 | Granular ferric hydroxides investigated in this study

#	Adsorbent material	Supplier	Grain size after rinsing [mm]	Point of zero charge [pH_{PZC}]	Specific surface [m^2/g]
GFH1	FerroSorp RW	HeGo Biotec	0.5–2.5	8.6	210
GFH2	FerroSorp Plus	HeGo Biotec	0.5–2.5	8.7	230
GFH3	Double P + S	BwF Brauchwasserfilter	1.25–2.5	8.5	242
GFH4	K24 Phosphatbinder	Teichpoint	2.24–8.0	8.3	279

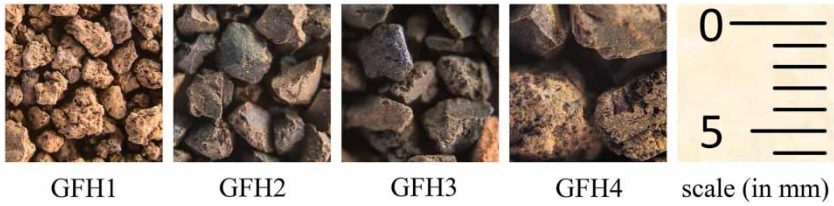

Figure 2 | Macro photographs of the different GFH adsorbents.

filtered into an empty glass bottle using a syringe with an attachable nylon filter (0.45 µm pore width). From the filtrate, total P and the pH (pH_{end}) were determined. The experiments were performed in a single approach, except for Experiment 4 (duplicate approach, i.e. two parallel runs), for which the results are presented as mean values with their standard deviations.

In Experiment 1, the NTMP adsorption behavior of four different GFH adsorbents was determined according to the procedure described above for a contact time (t_c) of 1 h and various pH values in order to identify the best performing material ($T = 20$ °C; pH 4, 6, 8, 10, and 12; $t_c = 60$ min; initial concentration = 1 mg/L NTMP-P; four different GFH adsorbents). It is noteworthy that this contact time was not sufficient to reach equilibrium. However, since Experiment 1 merely served to compare the adsorption behavior of the four different adsorbents, it was not necessary to reach equilibrium. In Experiment 2, a thermodynamic study of NTMP adsorption on GFH1 was carried out. For this, longer contact times (up to 7 d) were used to allow more time to reach a possible equilibrium. The influence of temperature on NTMP adsorption was investigated in the temperature range of 5–35 °C ($T = 5$, 20, 35 °C; pH 6; $t_c = 60$ min – 7 d; initial concentration = 1 mg/L NTMP-P; GFH1). Experiment 2 was carried out in rooms with different temperatures (climatic room 1 with cooling (5 °C), laboratory at room temperature (20 °C), and climatic room 2 with heating (35 °C)) to keep the temperature constant during the experiment. The experiments were not started until the solution had reached the respective room temperature. For Experiments 1 and 2, the initial NTMP concentration remained constant while the GFH dosages varied from 0.74 to 14 g/L in Experiment 1 and from 0.02 to 14 g/L in Experiment 2. In Experiment 3, the adsorption capacity of GFH1 for the six phosphonates and the influence of the pH on the adsorption of these compounds were investigated ($T = 20$ °C; pH 4, 5, 6, 7, 8, 9, 10, and 12; $t_c =$ 60 min; initial concentration = 1 mg/L HPAA-P, PBTC-P, HEDP-P, NTMP-P, EDTMP-P, and DTPMP-P; GFH1). Here, a constant factor of 0.23 g GFH1/µmol of P compound was applied. Experiment 4 investigated the regenerability of GFH1 in five cycles ($T = 20$ °C; pH 6; $t_c = 60$ min each for adsorption and desorption; $t_c =$ 15 min each for three rinsing steps; initial concentration = 1 mg/L NTMP-P; regeneration solution = 1 M NaOH; GFH1). After performing each adsorption step as described above, the supernatant (later to be filtered and analyzed) was decanted. For the desorption steps, the centrifuge tube was then filled with 1 M NaOH solution up to the 50 mL mark, rotated for 60 min, and decanted again (the decanted supernatant was analyzed as well). To remove NaOH residues which could have unintentionally increased the pH of the solution in the next adsorption step, the same procedure was repeated three times in a row with 50 mL of a buffer solution (0.01 M MES; pH 6) before the next cycle began. For both NaOH and buffered solution, fresh solutions were used in each cycle. The dry weight of GFH1 was determined before and after the five cycles to identify how much material had been lost in the experiment.

Analytical methods

A modified method based on ISO 6878 (ISO_{mini}, molybdenum blue method), as described by Rott *et al.* (2018c), was used for phosphorus analysis. The applicability of this method was confirmed using various organic buffers at 0.01 M mixed with 1 mg/L NTMP-P and 1 mg/L KH_2PO_4-P standard, at different $K_2S_2O_8$ (oxidizing agent) and NaOH doses and paralleled by P determinations according to ISO 6878 (Rott *et al.* 2018c). All glass materials that came into contact with the sample were thoroughly rinsed with hydrochloric acid (10%) and deionized water prior to the analysis. The digestion was carried out in a HachLange HT200S thermostat. The absorbance was measured with the UV/VIS spectrophotometer Nanocolor UV/VIS II from Macherey-Nagel. For the analysis of the strongly alkaline regeneration solution, the original ISO 6878 method (molybdenum blue

method) was used (ISO 6878:2004). The pH value was determined with the WTW pH electrode SenTix 81 in combination with the instrument WTW pH91. Scanning electron microscopy was applied using a Zeiss DSM-982 Gemini microscope with a thermal Schottky field emitter. For preparation, individual samples were applied to a sample carrier and fixed with conductive silver. To prevent electrical charging of the granules and to gain a clear image, the samples were sputtered with gold using a Leica coater (EM ACE 600). Furthermore, energy-dispersive X-ray spectroscopy (EDS) was performed with an X-ray detector from ThermoScientific (DSM-982 UltraDRY SDD detector).

Model equations

The Freundlich isotherms were modeled using Equation (1). The parameters K_F and n were determined by non-linear regression using the least-squares method.

$$q = K_F c^{1/n} \tag{1}$$

Additionally, the model by Langmuir (Equation (2)) was applied to the experimental data. The parameters q_{max} and K_L were determined by non-linear regression using the least-squares method.

$$q = q_{max} \frac{K_L c}{1 + K_L c} \tag{2}$$

All model parameters can be found in Table S1 (Supplementary Material). The Freundlich model led to the best r^2 values, and therefore, only Freundlich isotherms are shown in this study.

For the thermodynamic calculations, Equations (3) and (4) were used. By determining thermodynamic parameters such as the change in enthalpy (ΔH^0), entropy (ΔS^0), and free Gibbs energy (ΔG^0), it was possible to assess whether the sorption process is endothermic or exothermic as well as the strength and spontaneous nature of adsorption (Yan *et al.* 2015).

$$\Delta G^0 = -RT \ln K_d \tag{3}$$

$$\ln K_d = \frac{\Delta S^0}{R} - \frac{\Delta H^0}{RT} \tag{4}$$

In Equations (3) and (4), R is the universal gas constant (8.314459 J/(mol K)), T is the temperature (K), and K_d is the dimensionless form of the Freundlich constant. To make the temperature-dependent Freundlich constant K_F dimensionless, it was corrected by a factor of 1,000 g/L (density of water), as according to Milonjić (2007).

The enthalpy and entropy change was determined from the slope and intercept of the plot of ln K_d vs $1/T$, also known as the van 't Hoff plot. A positive value of ΔH^0 indicates endothermic adsorption, i.e. the adsorption process consumes energy. An exothermic adsorption is described by a negative value, which means that energy is released. Negative values of ΔG^0 describe an exergonic (spontaneous) adsorption, while positive values of ΔS^0 indicate that the randomness at the solid–solution interface increases during adsorption (Yan *et al.* 2010; Wasielewski *et al.* 2018).

The curves in Figure 6, plotting the adsorption capacity as a function of pH, were modeled by the logistic function model (Equation (5)). The parameters a, b, and d were determined by non-linear regression using the least-squares method.

$$c_{ads}(\mathrm{pH}) = 1 \frac{\mathrm{mg}}{\mathrm{L}} - \frac{d}{(1 + a e^{-b \times \mathrm{pH}})} \tag{5}$$

The coefficient of determination r^2 was calculated as according to Rott *et al.* (2018b). For the species distribution in Figure 6, the pK values from Rott *et al.* (2018b) were used. Additionally, pK values of 1.12, 3.48, 8.00, and 13.48 for HPAA were applied as calculated for 0 M ionic strength, as according to CA (2017).

To test the significance of the experimental and modeled data, a Student's t-test was performed. Calculated p-values can be found in Table S1 and Table S2 (Supplementary Material).

RESULTS AND DISCUSSION

Experiment 1 – effect of adsorbent nature on NTMP adsorption

Figure 3 enables a comparison of the adsorption behavior of the four GFH adsorbents examined at a 1 h contact time and different pH values. Since the pH of the solution shifted in the direction of the pH_{PZC} of the GFH during adsorption, the indicated pH ranges describe the ranges between pH_{start} and pH_{end}. All materials generally achieved higher loadings at lower pH values. The adsorbents show a positive net surface charge at pH values below the pH_{PZC}, which increases with increasing deviation from the pH_{PZC}. NTMP is negatively charged over the entire pH range tested so that adsorptive and adsorbent experience a stronger electrostatic attraction at lower pH values (Nowack & Stone 1999a).

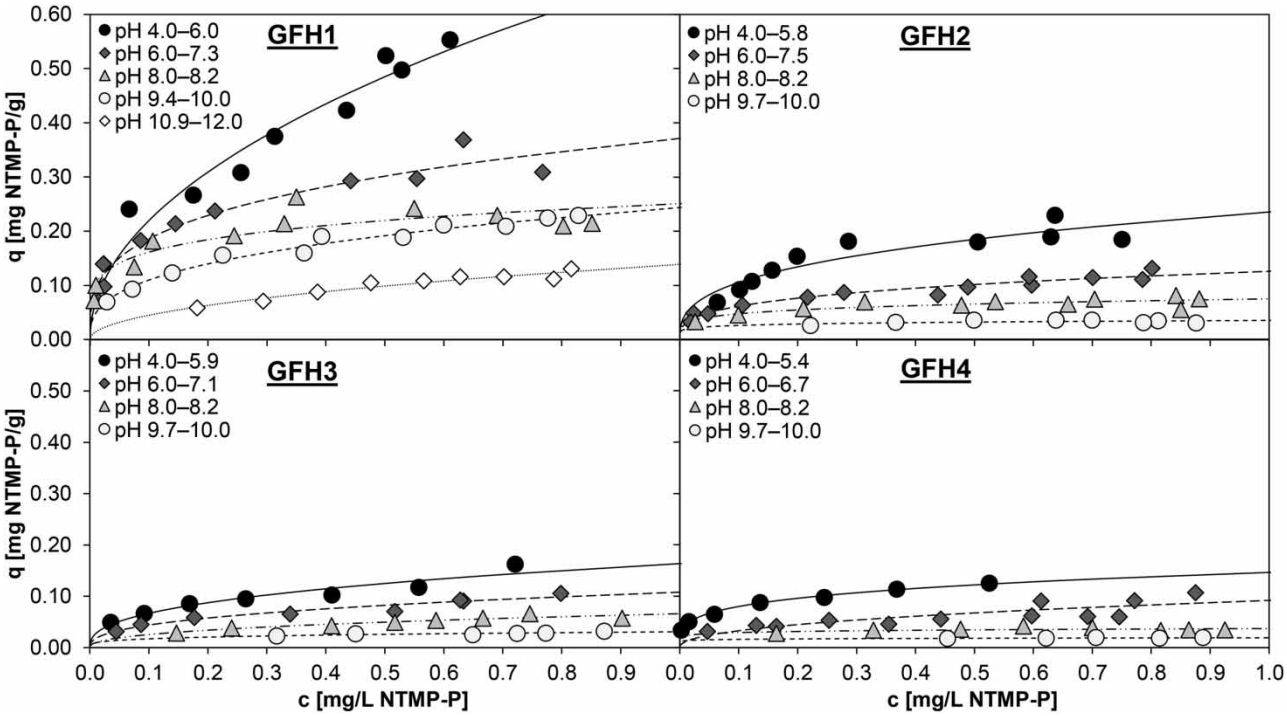

Figure 3 | Effect of adsorbent nature on NTMP adsorption with 1 mg/L NTMP-P depending on the pH (buffer: 0.01 M AcOH, 0.01 M MES, 0.01 M EPPS, 0.01 M CAPS) at room temperature (20 °C) (20 rpm, $t_c = 1$ h). Freundlich models are shown (model constants in Table S1, Supplementary Material).

GFH1 was the material with clearly the best performance. For instance, GFH1 achieved a loading of 0.55 mg NTMP-P/g at a pH of 4.0–6.0. In contrast, the second-best GFH (GFH2) had a maximum loading of only 0.23 mg NTMP-P/g. This loading was achieved by GFH1 even at the pH range of 9.4–10.0. Interestingly, GFH4 performed poorly in comparison despite the largest specific surface area (Table 1). Considering the pH_{PZC} of all investigated adsorbents was in a similar range, the choice of grain size plays a more important role in adsorption.

Two images depicting different sites of GFH1 at 20,000× magnification show that the material has a crystalline structure formed by crystals of different sizes, corroborating a high porosity (Figure 4). The EDS detected mainly Fe, O, and Ca (H is not detected by the EDS technique). The Ca has its origin in the production process in which calcium-containing compounds are used. Ca has been found to have a positive effect on the adsorption of phosphonates (Nowack & Stone 1999b; Boels *et al.* 2012), which could explain why GFH1 had a notably higher loading when compared with

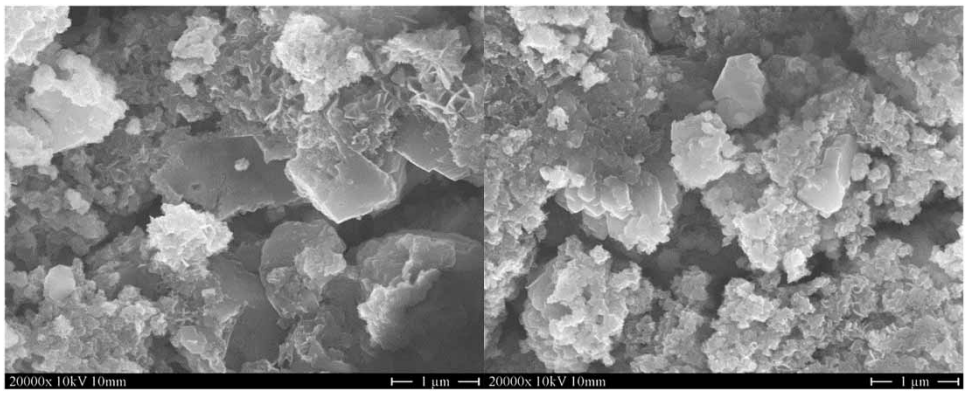

Figure 4 | Scanning electron microscope images of GFH1 at a magnification of 20,000×.

the other GFH adsorbents (≥12–19% $CaCO_3$ content in GFH1, for comparison in GFH2 only 5–10%).

Previous experiments (Figure S1, Supplementary Material) on the stability of the material with respect to the pH had shown that GFH1 was chemically unstable at pH <6, suggesting poor long-term applicability. Thus, the treatment of phosphonate-containing solutions with GFH1 is recommended to be performed at pH values close to 6, despite its remarkably higher short-term efficiency at pH <6. Since GFH1 proved to be the most efficient of the four GFH adsorbents, it alone was tested in the following experiments (2–4).

Experiment 2 – thermodynamics study of NTMP adsorption on GFH1

Additional isotherms with GFH1, the best-performing phosphonate in Experiment 1, were prepared at pH 6.0–7.8 and contact times of 1, 3, and 7 d (Figure 5 left). Except for the isotherm after 3 d ($r^2 = 0.713$), all could be well described with the Freundlich model ($r^2 \geq 0.847$; Table S1).

Since it is known from previous studies that the kinetics increase up to a certain limit with increasing mixing speed, it is likely that a higher agitation would allow faster achievement of equilibrium. Rout *et al.* (2014) showed that the percentage removal of phosphate by adsorption on red soil increased from 88.4% to about 96% when the rotational speed was increased from 100 rpm to 175 rpm. That said, it is not clear whether these experiments at low mixing speed were already in equilibrium after the contact time of 90 minutes. Lin *et al.* (2013) found that although agitation (varying from 0 to 200 rpm) had a considerable influence on the kinetics before equilibrium was reached, it had no noticeable influence on the adsorption of ammonium on zeolite at a 24-hour contact time. However, the influence of mixing speed was not investigated in this study, as the low speed of 20 rpm, chosen in analogy with the experiments of Laiti *et al.* (1995) at 30 rpm, was intended to avoid abrasion of the particles. The adsorbent should be kept as undamaged as possible in order to allow a better comparison with future column experiments, since it is known that the achievable adsorbent load for a given concentration depends on the particle radius of the adsorbent. Thus, isotherms determined with ground material may not accurately reflect the adsorption behavior of the original particles (Worch 2012). Therefore, even after 3 d, equilibrium was not reached. Isotherms not in equilibrium are empirical and any conclusions about a specific adsorption mechanism should be considered with care (Chen *et al.* 2017). However, it can be expected that isotherms gained at 7 d contact time were very close to equilibrium.

At an initial concentration of 1 mg/L NTMP-P, the maximum loading after 7 d was ~12 mg P/g. Experiments with an initial concentration of 5 mg/L NTMP-P and a pH of 6.0–8.0 resulted in a higher maximum loading of about 18 mg P/g (58 mg NTMP/g) due to the stronger gradient between NTMP and GFH1 (Figure S2, Supplementary Material). In similar investigations, but with a significantly higher initial concentration of 9.3 mg/L NTMP-P and a slightly higher pH of 7.85, Boels *et al.* (2012) found a maximum loading on GFH of ~22 mg NTMP-P/g. On the other hand, in similar conditions (9 mg/L NTMP-P, pH 8.3), Chen *et al.* (2017) found a much lower equilibrium loading of ~9 mg NTMP-P/g after 24 hours (not in equilibrium). Unfortunately, in these studies, the experiments were

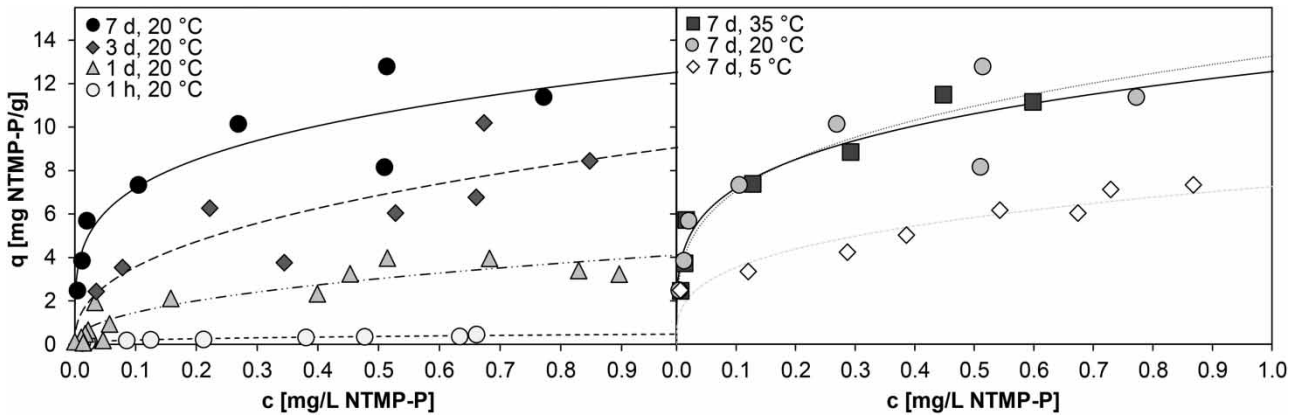

Figure 5 | Thermodynamics study of NTMP adsorption on GFH1 with 1 mg/L NTMP-P at an initial pH of 6 (buffer: 0.01 M MES) at different contact times (left) and different temperatures (right) (20 rpm). Freundlich models are shown (model constants in Table S1, Supplementary Material).

conducted at pH values at which GFH does not perform optimally, which is why no direct comparison is possible with the results of the current study.

At a temperature of 5 °C, the maximum loading was only ~7 mg P/g (Figure 5 right). Consequently, the adsorption performance was increased when thermal energy was applied. Wang *et al.* (2014) discovered the same behavior for the adsorption of phosphate on iron-coated activated carbon when investigating temperatures of 20, 30, and 40 °C. They explained that as the temperature in the water increases, the surface activity of the adsorbent increases as well. As a result, the interaction forces between adsorbent and adsorptive become stronger (Wang *et al.* 2014). That said, no difference in the maximum loading was found between the temperatures of 20 °C and 35 °C. Therefore, it was concluded that 12 mg P/g (39 mg NTMP/g) is the maximum possible loading of GFH1 at an initial concentration of 1 mg/L NTMP-P and 20 rpm.

The strikingly poorer performance of the adsorbent at low temperatures implies that low wastewater temperatures should be avoided in possible technical implementations for the adsorption of phosphonates on GFH. Therefore, the process is particularly suitable for industries that produce excess waste heat, which can be used to raise the temperature of the wastewater.

Table 2 shows the results of the thermodynamic calculations. The positive ΔH^0 value indicates an endothermic reaction due to pore size enlargement and/or activation of the adsorbent surface (Yan *et al.* 2010). In addition, the magnitude of ΔH^0 indicates the type of interactions that occur between adsorbent and adsorbate. Values for physisorption are usually below 20 kJ/mol, electrostatic interactions are indicated by a range of 20–80 kJ/mol, and chemisorption bond strengths can be from 80 to 450 kJ/mol (Bonilla-Petriciolet *et al.* 2017). Therefore, the adsorption of NTMP on GFH1 may be attributed to physisorption, i.e. the interactions between adsorbent and adsorbate can be dipole–dipole, hydrogen bonds, or van der Waals (Bonilla-Petriciolet *et al.* 2017). This is in line with the findings of Boels *et al.* (2010), who found a value of −10.5 kJ/mol for ΔG^0 and also derived physisorption for the adsorption of NTMP on a GFH. Using their density functional theory model, Martínez & Farrell (2017) found similar results. They concluded that the adsorption of NTMP to GFH is both physisorption, promoted by hydrogen bonding between O atoms in the NTMP and H atoms on the iron hydroxide, and chemisorption. They expect that the initially physically adsorbed NTMP is subsequently converted to chemically bound NTMP in a slower process. The negative values of ΔG^0 describe an exergonic adsorption, i.e. the adsorption occurs spontaneously. The positive value of ΔS^0 indicates that the randomness at the solid–solution interface increased during adsorption. Furthermore, it shows the affinity of NTMP towards GFH1 (Yan *et al.* 2010; Rout *et al.* 2015).

Table 2 | Thermodynamic data of NTMP adsorption on GFH1

T [K]	ΔG^0 [kJ/mol]	ΔH^0 [kJ/mol]	ΔS^0 [J/K/mol]
278	−20.6	14.5	126.7
293	−23.0		
308	−24.3		

Experiment 3 – effect of phosphonate nature and pH on GFH1 adsorption capacity

For all six phosphonates, as for NTMP, a decreasing adsorption behavior could be seen with increasing pH (Figure 6). In addition, a reduction of the adsorption affinity was associated with an increasing number of phosphonate groups (PG) and increasing molecular mass. PBTC deviated from this pattern slightly as, at pH <9, PBTC-P adsorbed in a similar ratio to HEDP-P despite a higher molecular mass than HEDP. For example, at pH 8, for HPAA (1 PG, 156.03 g/mol), PBTC (1 PG, 270.13 g/mol), HEDP (2 PG, 206.03 g/mol), NTMP (3 PG, 299.05 g/mol), EDTMP (4 PG, 436.12 g/mol), and DTPMP (5 PG, 573.20 g/mol), adsorption concentrations of 0.91, 0.84, 0.81, 0.58, 0.41, and 0.36 mg P/L and loadings of 3.92, 3.62, 3.44, 2.50, 1.74, and 1.55 μmol phosphonate/g GFH were found (according to model functions, Table S2).

The three largest molecules investigated all had similar functional groups in varying numbers (NTMP: one amino group, three methylene phosphonate groups; EDTMP: two amino groups, four methylene phosphonate groups; DTPMP: three amino groups, five methylene phosphonate groups), i.e. the molecular size increased in the following order: NTMP < EDTMP < DTPMP. Thus, the observed decrease of phosphonate adsorption with increased molecular size could be expected since larger molecules usually occupy more adsorption sites (Nowack & Stone 1999a). Furthermore, the more phosphonate groups a polyphosphonate has, the higher its negative charge becomes. When these highly negatively charged species adsorb, the adsorption of further phosphonate molecules is disturbed by the transfer of the negative charge to the surface (Nowack & Stone 1999a).

A slight variation in the pattern for PBTC was not extraordinary since this compound contains three carboxyl

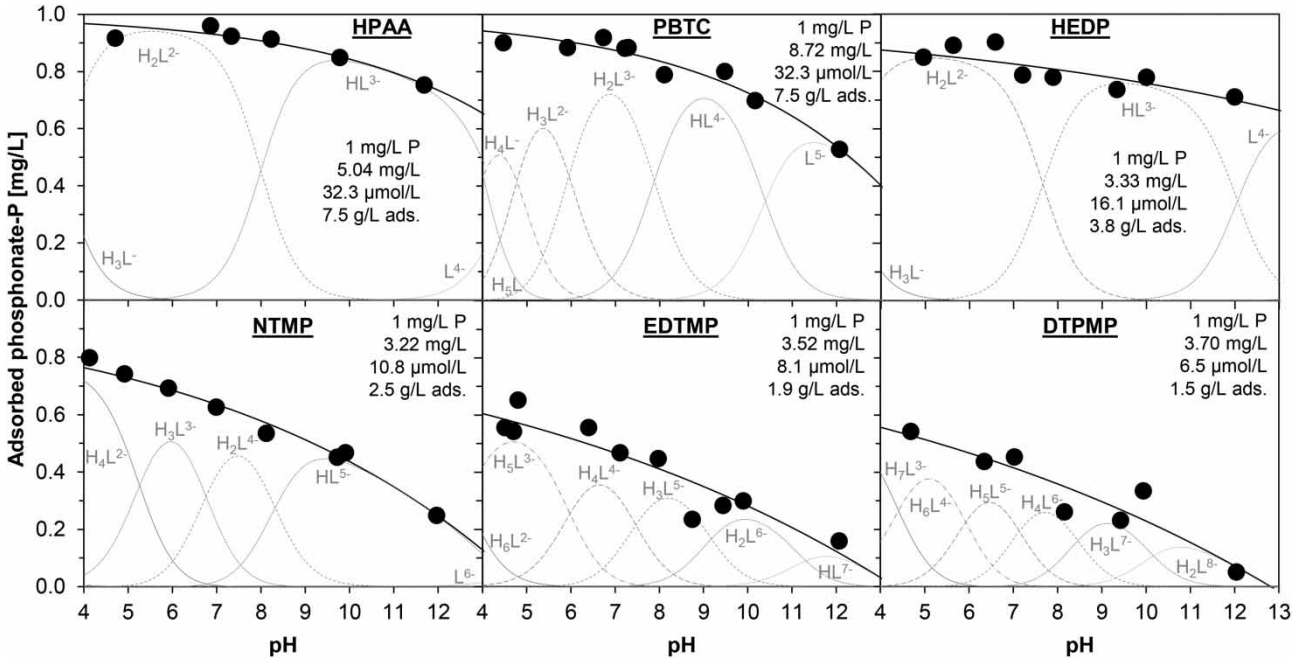

Figure 6 | Effect of phosphonate nature and pH on GFH1 adsorption capacity with a dosage of 0.23 g GFH1/µmol phosphonate at room temperature (20 °C) (20 rpm, $t_c = 1$ h). Solutions with 1 mg/L P, buffered at a pH of 4 and 5 (0.01 M AcOH), pH 6 (0.01 M MES), pH 7 (0.01 M MOPS), pH 8 (0.01 M EPPS), pH 9 (0.01 M CAPSO), and pH 10 and 12 (0.01 M CAPS) (model constants in Table S2, Supplementary Material).

groups (R-COOH), which are absent in the other phosphonates with the exception of HPAA (one carboxyl group). The deviation from the pattern, however, disappeared as soon as the fully deprotonated PBTC species became dominant at pH >9. Interestingly, there was still adsorption and no sudden drop of adsorption at pH values higher than the pH_{PZC} for all investigated phosphonates, meaning that adsorption also took place on the adsorbent with a negative net surface charge.

Similar findings regarding the influence of an increasing number of phosphonate groups were reported by Nowack & Stone (1999a, 2006) for phosphonate adsorption on goethite and by Rott *et al.* (2017a) and Klinger *et al.* (1998) for precipitation/flocculation experiments. It is also known that nitrogen-free phosphonates and aminophosphonates show a different behavior during ozonation experiments (Klinger *et al.* 1998; Xu *et al.* 2019). Therefore, if problems arise with the removal of phosphonates from phosphonate-containing solutions, it may be sufficient to substitute the corresponding phosphonate in the industrial process with another phosphonate that is easier to remove.

It is important to point out, however, that no final conclusions can be drawn from these experiments on real wastewater, as additional competing ions are present in a wastewater matrix. Phosphonate contaminated industrial wastewaters can be classified into two groups. The first group mostly comprises clear concentrates with low organic loads, high water hardness, and high anion concentrations (e.g. membrane concentrates and cooling wastewater). The second group consists of wastewater with high organic load, such as wastewater from paper and textile industries (Rott *et al.* 2017a). Especially in concentrates, high concentrations of calcium and magnesium can often be found (Sperlich *et al.* 2010; Antony *et al.* 2011; Chen *et al.* 2017). It is known from previous studies that calcium has a positive influence on the adsorption of phosphonates (Nowack & Stone 1999b; Boels *et al.* 2012). Boels *et al.* (2010) showed that anions such as carbonate and sulfate can also influence the adsorption of NTMP. Therefore, further experimentation with real wastewater and on the influence of other ions, which could compete or support phosphonate adsorption, has to be conducted to enable the transferability of the results to future technical realizations for the adsorption of phosphonates on GFH.

Experiment 4 – regenerability of GFH

Nowack & Stone (1999a) for goethite, as well as Boels *et al.* (2012) and Chen *et al.* (2017) for GFH adsorbents, have already investigated the desorption of NTMP, but only in one, two, and three cycles, respectively. Figure 7 shows that GFH1 could be loaded and unloaded several times

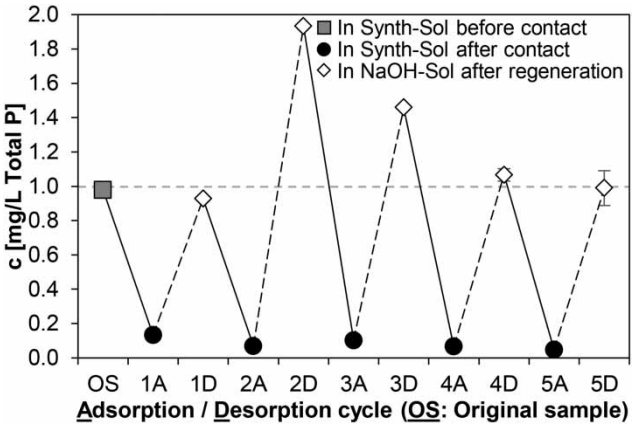

Figure 7 | Total P in synthetic solution (Synth-Sol) initially containing 1 mg/L NTMP-P before and after contact with 15 g/L GFH1 initially at pH 6 (0.01 M MES) as well as in 1 M NaOH solution (NaOH-Sol), and after regeneration of GFH1 for five adsorption (A) and desorption (D) cycles (20 °C, 20 rpm, $t_c = 1$ h, three rinsing steps for 15 min each with 0.01 M MES solution (pH 6) after each regeneration).

without loss of adsorption capacity. After each adsorption cycle, the total P concentration was ≤0.1 mg/L, resulting in a removal efficiency of ≥90%.

Total P concentrations >1 mg/L were found in the regeneration solutions, proving that GFH1 already contained phosphorus compounds which were desorbed during the desorption phases with 1 M NaOH solution together with the adsorbed NTMP. Interestingly, these concentrations >1 mg/L were first found after the second desorption (2D). After this cycle, the P concentration in the regeneration solutions continuously decreased and approached 0.99 mg/L P after five cycles. This may be due to a gradual leaching effect of the phosphorus present in the material, as fresh regeneration solution was always used in each desorption step. The fact that after the fifth adsorption step still a very low residual concentration of 0.05 mg/L P was found in the solution (5A) and the total P concentration in the regeneration solution was 0.99 mg/L (5D) indicates that all phosphorus contamination of GFH1 may be washed out, at the latest, by the fifth cycle.

The increase of the pH using a 1 M NaOH solution led to NTMP desorption which can be explained by electrostatic effects (Chen *et al.* 2017). During desorption, hydroxide ions from the NaOH solution interact with the adsorption sites and substitute in place of the adsorbed NTMP, which results in a significantly higher negative net surface charge (Zach-Maor *et al.* 2011). Additionally, the increase in pH results in an increase in the negative charge of NTMP ions (see Figure 6), leading to electrostatic repulsion. Future experiments should investigate multiple re-use of the regeneration solution.

In addition, by weighing the dry mass of the GFH before and after the experiment, it was determined that 38% of the initial concentration of 15 g/L GFH1 was lost during the five cycles. This was caused by abrasion of GFH1 into finer particles which were then removed partially with the supernatant. Although such a relatively high material loss was recorded, the NTMP removal rates were still high in all cycles, underlining the excellent performance of this material in adsorbing NTMP. Assuming this loss of material occurred linearly, and each desorption step was efficient in desorbing all NTMP, there would still be enough adsorbent (~6 g/L) to remove >90% P by the time the ninth cycle had been reached (according to the adsorption isotherm in Figure 3). However, such assumptions and calculations are unreliable, which is why batch experiments are only indicative experiments. For a higher accuracy, column tests that typically lead to less material loss should be carried out in the future.

CONCLUSIONS

This work showed that GFH could be used to remove all investigated phosphonates from water. For GFH1, the adsorption capacity decreased for all phosphonates with an increasing pH value, and for polyphosphonates, the adsorption capacity decreased with an increasing number of phosphonate groups. To achieve the best performance, the treatment of phosphonate-containing solutions should be carried out at pH values close to 6. Additionally, a temperature of 20 °C is adequate for the effective adsorption of NTMP onto GFH1. The treatment of phosphonate-containing solutions at low temperatures should be avoided, as the performance of phosphonate adsorption decreases with temperature. It was shown that phosphonates with different properties (molecular size and weight, number of phosphonate groups) behave differently during adsorption. Furthermore, five consecutive adsorption/desorption cycles were carried out showing high adsorption and desorption efficiency, indicating the possible re-usability of GFH1 for phosphonate removal. Finally, it needs to be tested with real wastewater to investigate the competing or supporting influence of other ions and in column experiments.

ACKNOWLEDGEMENTS

We acknowledge gratefully the Willy-Hager-Stiftung, Stuttgart, for their financial support. We also thank HeGo Biotec GmbH for providing adsorbent samples and

Zschimmer & Schwarz Mohsdorf GmbH & Co. KG for the supply of phosphonate samples.

SUPPLEMENTARY MATERIAL

The Supplementary Material for this paper is available at https://dx.doi.org/10.2166/wst.2020.055.

REFERENCES

Antony, A., Low, J. H., Gray, S., Childress, A. E., Le-Clech, P. & Leslie, G. 2011 Scale formation and control in high pressure membrane water treatment systems: a review. *Journal of Membrane Science* **383** (1–2), 1–16.

Armbruster, D., Rott, E., Minke, R. & Happel, O. 2019 Trace-level determination of phosphonates in liquid and solid phase of wastewater and environmental samples by IC-ESI-MS/MS. *Analytical and Bioanalytical Chemistry*. https://doi.org/10.1007/s00216-019-02159-5.

Boels, L., Tervahauta, T. & Witkamp, G.-J. 2010 Adsorptive removal of nitrilotris(methylenephosphonic acid) antiscalant from membrane concentrates by iron-coated waste filtration sand. *Journal of Hazardous Materials* **182** (1–3), 855–862.

Boels, L., Keesman, K. J. & Witkamp, G.-J. 2012 Adsorption of phosphonate antiscalant from reverse osmosis membrane concentrate onto granular ferric hydroxide. *Environmental Science and Technology* **46**, 9638–9645.

Bonilla-Petriciolet, A., Mendoza-Castillo, D. I. & Reynel-Ávila, H. E. 2017 *Adsorption Processes for Water Treatment and Purification*. Springer International Publishing, Cham, Switzerland.

CA 2017 Database of https://chemicalize.com (accessed 9 December 2017). ChemAxon Ltd.

Chen, Y., Baygents, J. C. & Farrell, J. 2017 Removing phosphonate antiscalants from membrane concentrate solutions using granular ferric hydroxide. *Journal of Water Process Engineering* **19**, 18–25.

Davenport, B., DeBoo, A., Dubois, F. & Kishi, A. 2000 *CEH Report: Chelating Agents*. Cited by Nowack, B. 2003 *Water Research* **37** (11), 2533–2546.

EPA 2013 *European Phosphonate Association – Phosphonates in Detergents*. EPA Detergent Phosphonates Dossier.

ISO 6878:2004 *Water Quality – Determination of Phosphorus – Ammonium Molybdate Spectrometric Method*. Beuth Verlag GmbH, Berlin, Germany.

Klinger, J., Sacher, F., Brauch, H.-J., Maier, D. & Worch, E. 1998 Verhalten organischer Phosphonsäuren bei der Trinkwasseraufbereitung (Behavior of organic phosphonic acids in drinking water treatment). *Vom Wasser* **91**, 15–27.

Kuhn, R., Jensch, R., Bryant, I. M., Fischer, T., Liebsch, S. & Martienssen, M. 2018 The influence of selected bivalent metal ions on the photolysis of diethylenetriamine penta(methylenephosphonic acid). *Chemosphere* **210**, 726–733.

Laiti, E., Öhman, L.-O., Nordin, J. & Sjöberg, S. 1995 Acid/base properties and phenylphosphonic acid complexation at the aged γ-Al_2O_3/water interface. *Journal of Colloid and Interface Science* **175** (1), 230–238.

Lesueur, C., Pfeffer, M. & Fuerhacker, M. 2005 Photodegradation of phosphonates in water. *Chemosphere* **59** (5), 685–691.

Lin, L., Lei, Z., Wang, L., Liu, X., Zhang, Y., Wan, C., Lee, D.-J. & Tay, J. H. 2013 Adsorption mechanisms of high-levels of ammonium onto natural and NaCl-modified zeolites. *Separation and Purification Technology* **103**, 15–20.

Martínez, R. J. & Farrell, J. 2017 Understanding nitrilotris(methylenephosphonic acid) reactions with ferric hydroxide. *Chemosphere* **175**, 490–496.

Matthijs, E., de Oude, N. T., Bolte, M. & Lemaire, J. 1989 Photodegradation of ferric ethylenediaminetetra(methylene-phosphonic acid) (EDTMP) in aqueous solution. *Water Research* **23** (7), 845–851.

Milonjić, S. K. 2007 A consideration of the correct calculation of thermodynamic parameters of adsorption. *Journal of the Serbian Chemical Society* **72** (12), 1363–1367.

Nowack, B. 2003 Environmental chemistry of phosphonates. *Water Research* **37** (11), 2533–2546.

Nowack, B. & Stone, A. T. 1999a Adsorption of phosphonates onto the goethite–water interface. *Journal of Colloid and Interface Science* **214** (1), 20–30.

Nowack, B. & Stone, A. T. 1999b The influence of metal ions on the adsorption of phosphonates onto goethite. *Environmental Science and Technology* **33** (20), 3627–3633.

Nowack, B. & Stone, A. T. 2006 Competitive adsorption of phosphate and phosphonates onto goethite. *Water Research* **40** (11), 2201–2209.

Rout, P. R., Bhunia, P. & Dash, R. R. 2014 A mechanistic approach to evaluate the effectiveness of red soil as a natural adsorbent for phosphate removal from wastewater. *Desalination and Water Treatment* **54** (2), 358–373.

Rout, P. R., Bhunia, P. & Dash, R. R. 2015 Effective utilization of a sponge iron industry by-product for phosphate removal from aqueous solution: a statistical and kinetic modelling approach. *Journal of the Taiwan Institute of Chemical Engineers* **46**, 98–108.

Rott, E., Minke, R. & Steinmetz, H. 2017a Removal of phosphorus from phosphonate-loaded industrial wastewaters via precipitation/flocculation. *Journal of Water Process Engineering* **17**, 188–196.

Rott, E., Minke, R., Bali, U. & Steinmetz, H. 2017b Removal of phosphonates from industrial wastewater with UV/Fe^{II}, Fenton and UV/Fenton treatment. *Water Research* **122**, 345–354.

Rott, E., Steinmetz, H. & Metzger, J. W. 2018a Organophosphonates: a review on environmental relevance, biodegradability and removal in wastewater treatment plants. *Science of the Total Environment* **615**, 1176–1191.

Rott, E., Nouri, M., Meyer, C., Minke, R., Schneider, M., Mandel, K. & Drenkova-Tuhtan, A. 2018b Removal of phosphonates from synthetic and industrial wastewater with reusable magnetic adsorbent particles. *Water Research* **145**, 608–617.

Rott, E., Reinhardt, T., Wasielewski, S., Raith-Bausch, E. & Minke, R. 2018c Optimized procedure for determining the adsorption of phosphonates onto granular ferric hydroxide using a miniaturized phosphorus determination method. *Journal of Visualized Experiments* **135**, e57618.

Sperlich, A., Warschke, D., Wegmann, C., Ernst, M. & Jekel, M. 2010 Treatment of membrane concentrates: phosphate removal and reduction of scaling potential. *Water Science and Technology* **61** (2), 301–306.

Wang, Z., Shi, M., Li, J. & Zheng, Z. 2014 Influence of moderate pre-oxidation treatment on the physical, chemical and phosphate adsorption properties of iron-containing activated carbon. *Journal of Environmental Sciences* **26** (3), 519–528.

Wasielewski, S., Rott, E., Minke, R. & Steinmetz, H. 2018 Evaluation of different clinoptilolite zeolites as adsorbent for ammonium removal from highly concentrated synthetic wastewater. *Water* **10** (5), 584.

Worch, E. 2012 *Adsorption Technology in Water Treatment: Fundamentals, Processes, and Modeling*. De Gruyter, Berlin, Germany.

Xu, Z.-B., Wang, W.-L., Huang, N., Wu, Q.-Y., Lee, M.-Y. & Hu, H.-Y. 2019 2-Phosphonobutane-1,2,4-tricarboxylic acid (PBTCA) degradation by ozonation: kinetics, phosphorus transformation, anti-precipitation property changes and phosphorus removal. *Water Research* **148**, 334–343.

Yan, L.-G., Xu, Y.-Y., Yu, H.-Q., Xin, X.-D., Wei, Q. & Du, B. 2010 Adsorption of phosphate from aqueous solution by hydroxy-aluminum, hydroxy-iron and hydroxy-iron–aluminum pillared bentonites. *Journal of Hazardous Materials* **179** (1–3), 244–250.

Yan, L.-G., Yang, K., Shan, R.-R., Yan, T., Wei, J., Yu, S.-J., Yu, H.-Q. & Du, B. 2015 Kinetic, isotherm and thermodynamic investigations of phosphate adsorption onto core–shell Fe_3O_4@LDHs composites with easy magnetic separation assistance. *Journal of Colloid and Interface Science* **448**, 508–516.

Zach-Maor, A., Semiat, R. & Shemer, H. 2011 Adsorption–desorption mechanism of phosphate by immobilized nano-sized magnetite layer: interface and bulk interactions. *Journal of Colloid and Interface Science* **363** (2), 608–614.

First received 26 November 2019; accepted in revised form 31 January 2020. Available online 11 February 2020